PROCEEDINGS OF SCIENCE

Forward Physics with the LHCf Experiment

Alessia Tricomi[*†]
University of Catania and INFN Catania, Italy
E-mail: alessia.tricomi@ct.infn.it

In 2016 the LHCf experiment has fulfilled its original goal of measuring the spectra of the neutral particles produced in the very forward direction at LHC at the highest energy ever available. The main purpose of these measurements is indeed to provide the Cosmic Ray and High Energy Physics communities with a missing unique set of information for the improvement of the hadronic interaction models used to simulate air showers development produced in the interaction of primary High Energy Cosmic Rays (HECR) with the Earth atmosphere. The last data sets collected by the LHCf experiment have been obtained during p+p collisions, at an energy of 13 TeV in the CM frame, and p+Pb collision, at an energy of 5.2 TeV and 8.1 TeV in the nucleon-nucleon CM frame. A review of the main results of LHCf and of the recent and on-going activities will be presented.

Sixth Annual Conference on Large Hadron Collider Physics (LHCP2018)
4-9 June 2018
Bologna, Italy

[*]Speaker.
[†]On behalf of the LHCf Collaboration

PoS(LHCP2018)207

1. Introduction

The knowledge of the hadronic interaction models is a key ingredient for a proper description of the properties of Ultra High Energy Cosmic Rays (UHECR). Indeed, despite the significant improvement in our understanding of UHECR properties thanks to the excellent performance of the giant hybrid arrays, like the Auger and TA experiments, still the results are largely affected by the poor knowledge of the nuclear interaction mechanism of primary cosmic rays with the Earth's atmosphere. In the analyses of observed data, comparison with Monte Carlo simulations of air showers is unavoidable, and the results are sensitive to the choice of hadronic interaction model used in the simulation [1]. Data collected at LHC provides a very important opportunity to calibrate the Monte Carlo codes used. Thanks to the LHC Run1 data, some interaction models have been updated, and the dispersion found in the predictions of air shower observables decreased. However, there is still significant difference between the model predictions especially in the forward region where particle production is particularly important since they carry a large fraction of collision energy and are responsible to determine the shape of air showers [2].

The Large Hadron Collider forward (LHCf) experiment was designed with the aim to provide a calibration of the hadronic interaction models in the whole energy range spanned by LHC by measuring the neutral forward particle produced in p-p as well as in p-Ion collisions. LHCf major objectives are to determine the differential production cross sections of photons, neutrons and neutral pions thus providing new information about high-energy hadronic interactions, due to its unique phase space coverage.

2. The LHCf experiment

The LHCf experiment is composed by two independent position sensitive electromagnetic calorimeters, located on both side of the ATLAS experiment, 140 m away from the LHC-IP1 interaction point, inside the zero-degree neutral absorber (Target Neutral Absorber, TAN). Charged particles from the IP are swept away by the inner beam separation dipole before reaching the TAN, so that only photons mainly from π^0 decays, neutrons and neutral kaons reach the LHCf calorimeters.

Each calorimeter (ARM1 and ARM2) has a double tower structure, with the smaller tower located at zero degree collision angle, approximately covering the region with pseudo-rapidity $\eta > 10$ and the larger one, approximately covering the region with $8.4 < \eta < 10$. The transverse dimensions of the calorimeters in Arm1 are 20 mm x 20 mm and 40 mm x 40 mm while they are 25 mm x 25 mm and 32 mm x 32 mm in Arm2. Each calorimeter is composed of 16 sampling scintillators and Tungsten plates for a total 44 radiation length thickness. Four X-Y layers of position sensitive detectors (scintillating fibers in ARM1, silicon micro-strip detectors in ARM2) provide measurements of the transverse profile of the showers. To improve the radiation hardness, sampling scintillators and scintillating fibers were replaced with GSO scintillators and GSO bars, respectively, from the operation of 2015 [3, 4]. The two tower structure allows to reconstruct the π^0 decaying in two γs, hitting separately the two towers, hence providing a very precise absolute energy calibration of the detectors. In the range E$>$ 100 GeV, the LHCf detectors have energy and position resolutions for

electromagnetic showers better than 5% and 200μm, respectively. A detailed description of the LHCf experimental set-up and of the expected physics performances can be found in Ref. [5, 6].

3. Recent results of LHCf

Since 2009 the LHCf experiment has collected data at different collision energies and with different colliding particles. Most operations were carried out with dedicated collision condition, i.e., under low luminosity to avoid pileup and high β^* to reduce the angular spread due to the beam divergence. Since 2015, the LHCf and ATLAS experiments have exchanged trigger informations with the aim to able to perform common analyses. In Table 3 a summary of the LHCf operations and analyses are reported.

Year	Energy [TeV]	Collisions	Detector	Papers		
				γ	n	π^0
2009-2010	0.9	p-p	ARM1 & ARM2	[7]		
2010	7		ARM1 & ARM2	[8]	[9]	[10, 11]
2013	2.76	p-p	ARM1 & ARM2			[11, 12]
2013	5.02	p-Pb	ARM2			[11, 12]
2015	13	p-p	ARM1 & ARM2	[13, 14]	[15]	
2016	5.02	p-Pb	ARM2			
2016	8.16	p-Pb	ARM2			

Table 1: Summary of the LHCf runs at LHC and analisys matrix.

3.1 Single photon spectra in p-p collisions at 13 TeV

The LHCf experiment has recently published the inclusive energy spectra of photons produced in p-p collisions at 13 TeV [13]. The spectra obtained in two pseudorapidity ranges are compared with the predictions of DPMJET 3.06 [16], EPOS-LHC [17], PYTHIA 8.212 [18], QGSJETII-04 [19] and SIBYLL 2.3 [20] hadronic interaction models, as shown in Fig. 1.

The results at 13 TeV confirms what has been already reported at lower energies.The LHCf data lie between MC predictions but there is not an unique model with a good agreement in the whole energy range and in both rapidity regions. In the pseudorapidity range $\eta > 10.94$, QGSJET and EPOS presents a good overall agreement with experimental data; SIBYLL predicts a lower yield of photons, even if it features a shape similar to data; PYTHIA spectrum agrees with data up to 3.5 TeV but becomes harder at higher energies; DPMJET is generally harder than data. In the pseudorapidity range $8.81 < \eta < 8.99$, EPOS and PYTHIA spectra agree with data up to 3 TeV, while they become harder at higher energies; SIBYLL has a good agreement up to 2 TeV, then also it becomes harder than data; QGSJET presents a lower yield of photons, while DPMJET generally predict an harder spectrum than experimental data.

A deeper study of the discrepancy has brought to the conclusion that the main differences between data and models were attributable to a less-than-complete understanding of the soft hadronic interactions implemented in the models as diffractive processes [21, 22]. Diffractive processes have a smaller multiplicity and produces more high-energy particles than non-diffractive processes.

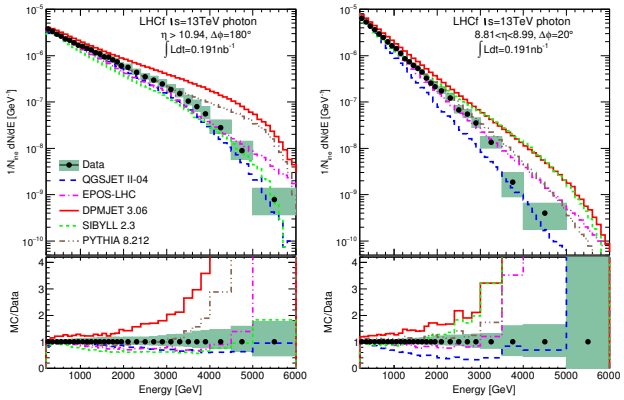

Figure 1: Inclusive photon energy spectra for pseudorapidity region $\eta > 10.94$ (left) and $8.81 < \eta < 8.99$ (right). Data are represented by black points while MC prediction from several models are represented by coloured histograms. Green shaded area represents statistical+systematic errors of data. Spectra are normalized to the total number of inelastic collisions. Bottom panels show the ratio of MC predictions to data.

LHCf alone is not able to distinguish diffractive events from other process, however, by combining the information collected by LHCf with the activity in the central ATLAS detector, it is possible to disentangle the diffractive contribution. ATLAS and LHCf had a common data taking both in the p-Pb runs as well in 13 TeV p-p operation. In these runs, ATLAS recorded data when LHCf observed high-energy particles in its detectors.

By using the information on the number of charged particles in the ATLAS central tracker, LHCf may classify its photon events as diffractive-like if no charged particles is identified in ATLAS and non-diffractive-like events when there is activity in the ATLAS tracker [14].

Fig. 2 (top) shows photon cross sections in the $\eta > 10.94$ (left) and $8.81 < \eta < 8.99$ (right) range for inclusive (filled circles) and diffractive-like (filled squares) events. As expected, the diffractive events exhibit a harder spectrum than the inclusive events. Predictions from various generators are also shown for two event categories. It is found that PYTHIA (orange lines) overpredicts the diffractive photons while the QGSJET (blue) and SIBYLL (green) strongly suppress. The relative production rates of diffractive-like events to the inclusive events are shown in Fig. 2 (bottom) together with the predictions of the Monte Carlo generators. EPOS (magenta) shows best agreement with data both in the absolute value and the energy dependence.

3.2 Inclusive neutron spectra at $\sqrt{s} = 13$ TeV

p-p collisions data at $\sqrt{s} = 13$ TeV have also been analyzed in order to measure the inclusive neutron production spectra. Currently, only the ARM2 detector have been used for such analysis and the differential cross section measured in three different rapidity regions, $\eta > 10.76$, $8.99 < \eta < 9.22$ and $8.81 < \eta < 8.99$, after unfolding the detector response, is shown in Fig. 3 together with the predictions of several Monte Carlo generators. The obtained results seems to confirm the same trend observed by LHCf in the 7 TeV data [9]. In particular, the peak at 0-degree for energy $\simeq 5.5$ TeV in the data is reproduced only qualitatively by the QGSJET II-04 model while

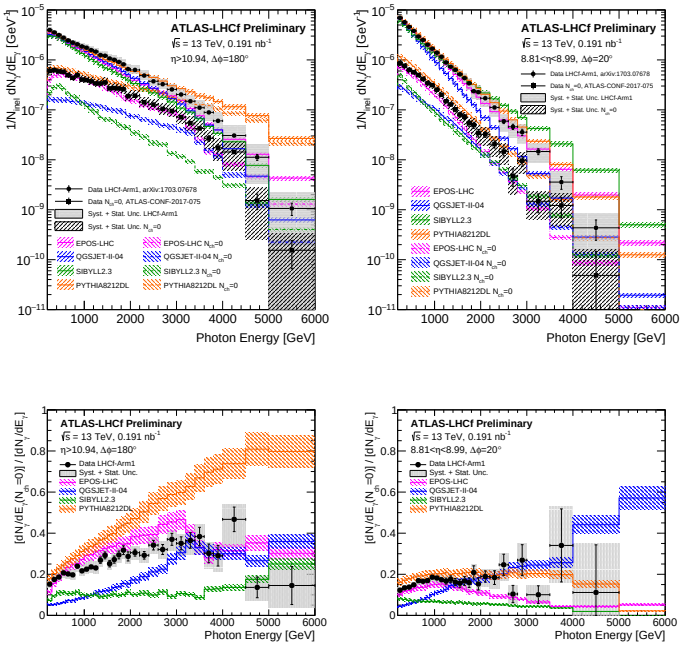

Figure 2: Forward photon energy spectra for inclusive and diffractive-like events (top) and ratio of diffractive-like to inclusive photons (bottom) for pseudorapidity region $\eta > 10.94$ (left) and $8.81 < \eta < 8.99$ (right). Data are represented by black points while MC prediction from several models are represented by coloured histograms. Grey shaded area represents statistical+systematic errors of data.

all the other models significantly underpredict the LHCf results. Results at lower rapidity are in better agreement with the model predictions than at high rapidity. In particular, SIBYLL 2.3 best reproduces the absolute cross section. This was not the case in the comparison between LHCf 7 TeV results wih previous SIBYLL version (2.1) [9]. The improvement of SIBYLL is also found in the $\eta > 10.76$ region.

Extensions of the results enlarging the phase space coverage by using also ARM1 data and by analyzing data taken at different detector position are ongoing.

4. Inclusive photon spectra in p-Pb collisions at $\sqrt{s} = 8.16$ TeV

In addition to the measurement performed in p-p collisions, LHCf has also taken data during 2016 in p-Pb run at the center-of-mass collision energy per nucleon of $\sqrt{s_{NN}} = 5.02$ and 8.16 TeV. Only the ARM2 detector was used for the operations, with the detector located on the p-remnant side. The measurements at the proton remnant side of p-Pb collisions at the LHC provide a unique tool to study the nuclear effect in the forward particle production which is particularly important for HECR Physics since the interactions of the primary cosmic rays in the atmosphere occur between proton and nucleus or between nucleus and nucleus, where one of the nucleus is light component. Analysis of the data collected is just started and the preliminary single photon inclusive spectra is shown in Fig. 4 in the pseudorapidity range $\eta > 10.94$ (left) and $8.81 < \eta < 8.99$ (right). Spectra

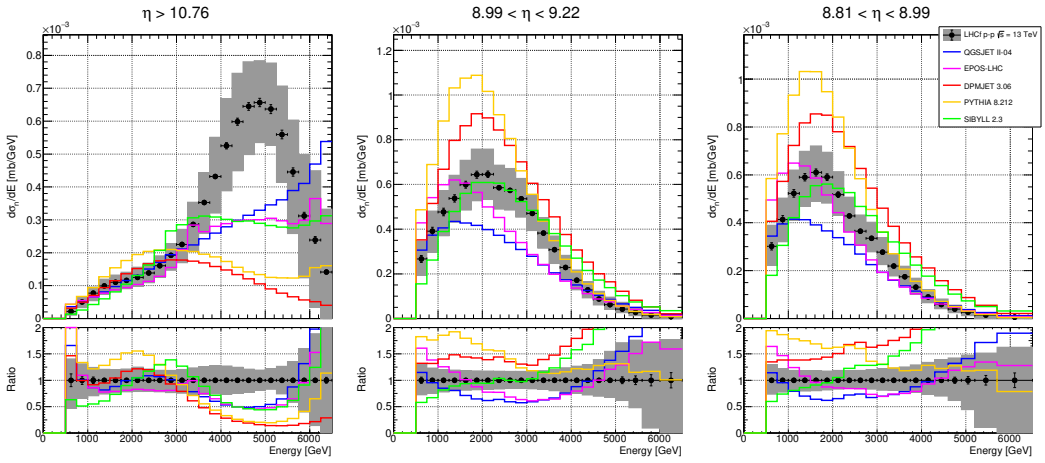

Figure 3: Inclusive neutron energy spectra of ARM2 detector for pseudorapidity region $\eta > 10.76$ (left), $8.99 < \eta < 9.22$ (center) and $8.81 < \eta < 8.99$ (right). Data are represented by black points while MC prediction from several models are represented by coloured histograms. Grey shaded area represents statistical+systematic errors of data. Spectra are normalized to the total number of inelastic collisions. Bottom panels show the ratio of MC predictions to data.

are currently normalized to the area above 200 GeV. Results are compared with the prediction of DPMJET 3.06 (red), QGSJETII-04 (blue) and EPOS (magenta) predictions.

5. Conclusions

Data collected by the LHCf experiment at various collision conditions at LHC provides an important set of information to calibrate the hadronic interaction models in the before-unexplored forward region relevant to constrain the particle production in high energy Cosmic Ray air shower.

Inclusive cross sections of photons, neutrons and π^0 at various conditions have been already published and they are used to update the hadronic interaction models. The discrepancy found between data and models may be related to the diffractive/non-diffractive components and may benefit of combined analysis between LHCf and ATLAS which is currently ongoing. In addition, the comparisons between the data at different collision energies reveal the scaling or scaling break of the particle spectra. The LHCf results indicate the scaling of photons and π^0 spectra at $\sqrt{s}$ =2.76, 7 and 13 TeV, while the ISR, PHENIX and LHCf seem to indicate a scaling break of neutron spectra between 200 GeV and 13 TeV. A new experiment, RHICf, has hence been prepared to test the scaling (or break) at $\sqrt{s} = 510$ GeV at RHIC. The experiment uses one of the LHCf detector, ARM1, and has taken data at the end of June 2017. Results from RHICf are coming and will bring further important information for Cosmic Ray physics.

References

[1] K.-H. Kampert and M. Unger, Astropart. Phys. **35** (2012) 660.

[2] K. Akiba et al., J. Phys. G: Nucl. Part. Phys. **43** (2016) 110201.

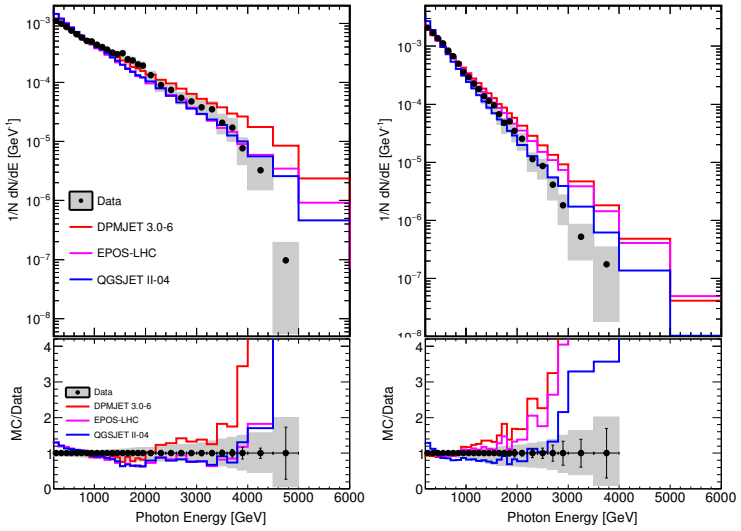

Figure 4: Preliminary inclusive photon spectra measured by LHCf in p-Pb collisions at $\sqrt{s_{NN}} = 8.16$ TeV in the pseudorapidity range $\eta > 10.94$ (left) and $8.81 < \eta < 8.99$ (right). Results are compared with the predictions of DPMJET 3.06 (red), QGSJETII-04 (blue) and EPOS (magenta).

[3] K. Kawade et al., JINST, **6** T09004 (2011).

[4] T. Suzuki et al., JINST, **8** T01007 (2013).

[5] The LHCf Collaboration, O. Adriani et al., JINST **3** (2008) S08006.

[6] The LHCf Collaboration, O. Adriani et al., International. J. of Mod. Phys. A **28** 1330036 (2013).

[7] O. Adriani et al., Phys. Lett. B **715** (2012) 298.

[8] O. Adriani et al., Phys. Lett. B **703** (2011) 128.

[9] O. Adriani et al., Phys. Lett. B **750** (2015) 360.

[10] The LHCf Collaboration, Phys. Rev. D **86** 092001 (2012).

[11] The LHCf Collaboration, Phys. Rev. D **94** 032007 (2016).

[12] The LHCf Collaboration, Phys. Rev. C **89** 065209 (2014).

[13] The LHCf Collaboration, Phys. Lett. B **780**, 233-239 (2018).

[14] The ATLAS and LHCf Collaborations, ATLAS- CONF-2017-075 (2017).

[15] The LHCf Collaboration, CERN-EP-2018-239; arXiv:1808.09877v1 [hep-ex].

[16] F.W. Bopp et al., Phys. Rev. **C77** (2008) 014904.

[17] K. Werner et al., Nucl.Phys.Proc.Suppl. **175-176** (2008).

[18] T. Sjöstand, et al., Comput. Phys. Comm. **178** (2008) 852.

[19] S. Ostapchenko, Phys. Rev. **D83** (2011) 014108.

[20] E.-J. Ahn et al., Phys. Rev. **D80** (2009) 094003.

[21] The ATLAS and the LHCf Collaborations, ATL-PHYS-PUB-2015-038.

[22] Q.D. Zhou, Y. Itow, H. Menjo and T. Sako, Eur. Phys. J. **C 77** (2017) 212.